Molecular Plant Pathology

XacFhaB adhesin, an important *Xanthomonas citri* subsp. *citri* virulence factor, is recognized as a pathogen-associated molecular pattern

Journal:	*Molecular Plant Pathology*
Manuscript ID:	Draft
Manuscript Type:	Original Article
Date Submitted by the Author:	n/a
Complete List of Authors:	Garavaglia, Betiana; IBR-CONICET-UNR, Zimaro, Tamara; IBR-CONICET-UNR, Abriata, Luciano; IBR-CONICET-UNR, Ottado, Jorgelina; IBR-CONICET-UNR, Gottig, Natalia; IBR-CONICET-UNR,
Keywords:	Non-fimbrial adhesin, Xanthomonas, citrus canker

XacFhaB adhesin, an important *Xanthomonas citri* subsp. *citri* virulence factor, is recognized as a pathogen-associated molecular pattern

Betiana S. Garavaglia, Tamara Zimaro, Luciano A. Abriata, Jorgelina Ottado[*] and Natalia Gottig[*]

[1]Instituto de Biología Molecular y Celular de Rosario, Consejo Nacional de Investigaciones Científicas y Técnicas (IBR-CONICET) and Facultad de Ciencias Bioquímicas y Farmacéuticas, Universidad Nacional de Rosario. Ocampo y Esmeralda, Rosario, 2000, Argentina.

LAA's current address: Laboratory for Biomolecular Modeling, School of Life Sciences, École Polytechnique Fédérale de Lausanne (EPFL), and Swiss Institute of Bioinformatics (SIB), AAB011 Station 19, 1015, Lausanne, Switzerland.

[*]To whom correspondence should be addressed at: Instituto de Biología Molecular y Celular de Rosario, Consejo Nacional de Investigaciones Científicas y Técnicas (IBR-CONICET). Ocampo y Esmeralda, Rosario, 2000, Argentina. Tel/Fax: +54 341 4237500. E-mail: ottado@ibr-conicet.gov.ar, gottig@ibr-conicet.gov.ar

Running Title: XacFhaB adhesin elicits plant defense responses

Keywords: Non-fimbrial adhesin, Xanthomonas, citrus canker

Word count: 5707

SUMMARY

Adhesion to host tissue is one of the key steps of the bacterial pathogenic process. *Xanthomonas citri* subsp. *citri* has a non-fimbrial adhesin protein XacFhaB required for bacterial attachment, which we have previously demonstrated that is an important virulence factor for the development of citrus canker. XacFhaB is a 4,753 residue long protein with a predicted β-helical fold structure, involved in bacterial aggregation, biofilm formation and adhesion to the host. In this work, to further characterize this protein and considering its large size, XacFhaB was dissected into three regions based on bioinformatic and structural analyses, for functional studies. First, the capacity of these protein regions to aggregate bacterial cells was analyzed. Two of these regions were able to form bacterial aggregates, being the most amino-terminal region dispensable for this activity. Moreover, XacFhaB has features resembling pathogen-associated molecular patterns (PAMPs), which are recognized by plants. As PAMPs activate plant basal immune responses, the role of the three XacFhaB regions as elicitors of these responses was investigated. All adhesin regions were able to induce basal immune responses in host and non-host plants, with a stronger activation by the carboxyl-terminal region. Furthermore, pre-infiltration of citrus leaves with XacFhaB regions impaired *X. citri* subsp. *citri* growth, confirming the induction of defense responses and restraint of citrus canker. This work reveals that adhesins from plant pathogens trigger plant defense responses, opening new roads for the development of protective strategies for disease control.

INTRODUCTION

Xanthomonas citri subsp. *citri* (Xcc) is a gram-negative plant pathogenic bacterium responsible for citrus canker. This disease is distributed worldwide and in severe cases causes economic losses due to plant defoliation, twig dieback, premature fruit drop and general debilitation of the tree (Graham *et al.*, 2004). Bacterial proteins related to attachment are important pathogenicity factors since adhesion to host tissues is a key step for plant colonization and disease development. We have determined that a non-fimbrial adhesin of Xcc named XacFhaB is an important virulence factor for the development of citrus canker. The expression of this adhesin was found to be induced *in planta* during canker development. This adhesin is necessary for attachment to plant surfaces, epiphytic fitness and colonization of citrus leaves, and is involved in cell-to-cell-attachment and biofilm formation (Gottig *et al.*, 2009).

XacFhaB is a 4,753-aa protein encoded by XAC1815 that has high amino acid homology to FhaB from *Bordetella pertussis* (Gottig et al., 2009) which is secreted by the two-partner secretion (TPS) pathway. FhaB has a signal peptide followed by the conserved `TPS domain´ that directs its secretion through its TPS partner named FhaC. Beyond the TPS domain, FhaB has a predicted structure of an elongated β-helix in which the β-helical fold continues as a rod-like structure ~500 Å long (Clantin *et al.*, 2004, Kajava *et al.*, 2001). The accepted model of FhaB secretion establishes that the N-terminus of FhaB recognizes the N-terminal domain of FhaC and then remains associated with it while the rest of the protein is translocated through the channel. During secretion, the carboxyl-terminus of FhaB is processed at the amino acid 3,528 generating a ~230 kDa mature protein. The mature form of FhaB is anchored to the outer membrane though the interaction with FhaC exposing the carboxyl-terminus domain (Mazar & Cotter, 2006, Noel *et al.*, 2012). It was demonstrated that this region

mediates adherence to epithelial and macrophage-like cells in animals and is required for colonization of host tissues and modulation of the inflammatory response (Julio *et al.*, 2009). To our knowledge no studies have been performed to infer plant pathogen non-fimbrial adhesin domains involved in adherence.

In human bacterial pathogens, there is an emerging idea that adhesins modulate the host immune response. In *Porphyromonas gingivalis*, a bacterial pathogen associated with several forms of chronic marginal periodontitis, long fimbrial adhesins interact with host-cell receptors and initiate intracellular signaling cascades leading to innate defense responses (Amano, 2010). And, specifically in the case of FhaB of *B. pertussis*, it has been observed that this adhesin activates the host interferon type I response (Dieterich & Relman, 2011). Also, it is widely known that *B. pertussis* FhaB is able to trigger an immune defense response in their hosts, and is in fact used in vaccination as an immunogenic molecule (Pines *et al.*, 1999, Sato & Sato, 1999). However, the role of this family of adhesins in plant immune responses has been only recently studied for a small filamentous hemagglutinin-like protein (Fha1) of *Xanthomonas campestris* pv. *vesicatoria* (Xcv) (Choi *et al.*, 2013). This protein is only 445-amino acids long and lacks the signal peptide and TPS domain. Fha1 interacts with *Capsicum annuum* hypersensitive induced reaction protein (CaHIR1), a pepper plasma membrane-localized protein that has been proposed to induce immunity-associated cell death (Choi et al., 2013). Pathogen-associated molecular patterns (PAMPs) generally are highly conserved molecules within a class of microbes that have an essential function in microbial fitness or survival. Plants have evolved the capacity to recognize these PAMPs though specific receptor triggering a first line of defense known as pattern-triggered immunity (PTI). PTI restricts pathogen growth and thus hampers tissue colonization (Chisholm *et al.*, 2006). The non-fimbrial adhesins such as XacFhaB

are important pathogenicity factors conserved in several plant and mammalian pathogens suggesting that they can act as PAMPs (Mhedbi-Hajri *et al.*, 2011).

To gain insights about the role of this family of adhesins and taking into account that XacFhaB is a large protein, in this work we expressed and purified different regions of this protein, and tested their functionalities in order to unveil the regions responsible for bacterial adhesion and to characterize if plants can recognize them as molecules capable of inducing defense responses.

RESULTS

XacFhaB triggers plant defense responses

In order to analyze whether XacFhaB could trigger plant defense responses, the transcript levels of several genes related with plant defense responses in citrus canker (Garavaglia *et al.*, 2010) were analyzed in citrus plants infiltrated with Xcc wild type and the ΔfhaB mutant. Plant RNA was extracted from citrus leaves 24 hour post-infiltration (hpi) and real-time quantitative reverse-transcriptase polymerase chain reactions (RT-qPCR) were performed. Several genes were analyzed: oxidative stress marker genes, such as *PEROXIREDOXIN* (*PrxA*), *NADPH OXIDASE* (*RbohB*), *GLUTATHIONE-S-TRANSFERASE* (*GST*) and *SUPEROXIDE DISMUTASE* (*SOD*); and defense response related genes including: *MITOGEN ACTIVATED PROTEIN KINASE 3* (*MAPK3*), *MAP KINASE KINASE 4* (*MKK4*), *WRKY30* transcription factor, *LIPOXYGENASE 2* (*Lox2*), *PATHOGENESIS RELATED 1* (*PR1*), *PR3* and *PR4*. RT-qPCR analysis showed that all transcripts but *Lox2* were significantly ($p < 0.05$) less abundant at 24 hpi in plants infected with the ΔfhaB mutant than in plants infected with Xcc wild type (Fig. 1).

Analysis and structural modeling of XacFhaB sequence and functional domains

XacFhaB is a large 4,753 amino acids protein with a calculated molecular weight of approximately 471 kDa. Like other hemagglutinin proteins, it has a signal peptide followed by a conserved TPS domain and then by a number of filamentous hemagglutinin repeats predicted to form a repetitive β-strand structure (Gottig et al., 2009). More precisely, PFAM domain annotation indicates that XacFhaB is composed of an amino-terminal region with several type-1 hemagglutinin repeats within the first ~3,400 residues, followed by a ~600 residue-long region of type-2 hemagglutinin repeats and finally by a ~700 residue-long C-terminal region that does not match any known domain (Fig. 2a). According to PFAM, the segments that separate hemagglutinin domains are rich in low-complexity regions, often involved in creating flexible hinges and in unspecific binding to other molecules (Coletta *et al.*, 2010, Rado-Trilla & Alba, 2012).

Secondary structure and disorder predictions suggest that the TPS (first ~300 residues) is well structured in the form of several short, consecutive β-strands, as observed indeed in the X-ray structure of the TPS from *B. pertussis* FHA (Clantin et al., 2004). The following ~2,800 residues (*i.e.* up to residue ~3,100) are predicted to have a large β content too, but also a disorder probability higher than that of well-folded domains yet below the threshold for disorder. This suggests a long, flexible but ordered β-structure scaffold. The region spanning residues 3,100 to 3,400 is predicted to be quite ordered, and is almost identical (97 % similar and 95 % identical) to the already studied Fha1 from Xcv (Choi et al., 2013) (Fig. S1, see Supporting Information). Finally, the last ~1,350 residues (starting at position ~3,400) include most of the type-2 hemagglutinin domains and are predicted to be largely disordered, especially those from ~3,500 till ~4,300.

Modeling the first 3,400 residues of XacFhaB with I-TASSER (Roy *et al.*, 2010, Yang *et al.*, 2015, Zhang, 2008) suggests a long β-helix structure that basically extends the TPS' β-helix fold from its C-terminus. Therefore, in summary, XacFhaB would be an extended, flexible β-helix with several type-1 hemagglutinin features up to residue 3,400-3,500, and a disordered structure with type-2 hemagglutinin features after that (Fig. 2b, c). Assuming a continuous β-helix structure for the full folded segment until residue 3,500, this would make up a filament-like structure around 35-45 Å thick and around 600 Å (0.6 μm) long when extended, a size similar to that proposed for *B. pertussis* FhaB from modeling and electron microscopy data (40 x 500 Å, (Kajava et al., 2001)). Interestingly, the sequence segment PLFETRIKFID in XacFhaB, which is cleaved in *B. pertussis* FhaB to achieve the final mature form (Noel et al., 2012), is conserved in XacFhaB between positions 3,542-3,550, *i.e.* right C-terminal to the last structured region. Such maturation point for XacFhaB would imply (i) the full exposition of the last folded segment (including all the type-1 hemagglutinin domains and the Fha-1-like region), and (ii) the release of a disordered polypeptide of ~1,200 residues with type-2 hemagglutinin signatures. These domains have not been much characterized but they compose a family of secreted bacterial exotoxins (InterPro025157).

Breaking down XacFhaB into three main regions for functional studies

Taking into account the analysis of XacFhaB sequence presented above (Fig. 2) and considering that it is a large protein difficult to be expressed completely in *E. coli* as a recombinant protein, we divided the protein in three polypeptides, named AR (Adhesin Region) 1 to 3: AR1 from amino acid 454 to 999 (53 kDa); AR2 from 1,113 to 1,613 (48 kDa); and AR3 from 2,324 to 3,046 (72 kDa). AR1 comprises the region right C-

terminal to the TPS domain and covers most of the first large series of type-1 hemagglutinin domains. Right after AR1, partially overlapping with the second large series of type-1 hemagglutinin domains, there is a long region made up of two large repeats that are 46 % identical (62 % similar) to each other (Fig. S1, see Supporting Information). Our AR2 region corresponds to the first of these two repeats. Finally, AR3 begins after the second repeat-like region of AR2 and finishes before the more ordered region highly homolog to the already studied Fha1 from Xcv (Choi et al., 2013). Together, AR3 and the subsequent Fha1-like segment comprise a region that in *B. pertussis* FhaB was proposed to be its most exposed part (Noel et al., 2012).

AR2 and AR3 regions of XacFhaB promote bacterial aggregation

The three XacFhaB regions were expressed as recombinant proteins in *Escherichia coli* and purified to homogeneity fused to a 6XHis-Tag. First, the ability of each AR region to aggregate bacterial cells was analyzed. This was evaluated using a GFP-expressing Xcc strain cultured in XVM2 in the presence of AR1, AR2 and AR3. The different proteins were incubated at 5 μM with the bacterial suspensions for 3 h and visualized by confocal microscopy. As a control, the bacterial suspensions were incubated for 3 h with 5 μM 6XHis-Trx that was purified in the same conditions as AR1, AR2 and AR3. The incubation with AR2 and AR3 caused a bacterial association similar to macrocolonies, effect not observed either in the incubations with AR1 or the control (Fig. 3). The ability of AR1, AR2 and AR3 to promote bacterial aggregation was also analyzed with the ΔfhaB mutant strain (Gottig et al., 2009) and results similar to Xcc wild type were obtained (data not shown). To notice was the fact that when the proteins were boiled 10 min in order to denature them, no agglutination was observed in any case, suggesting that a structured folding is required for this activity. The proteins were checked

by SDS-PAGE after denaturing to ascertain that the heat treatment did not degrade them (data not shown).

XacFhaB regions elicit plant defense responses when infiltrated

The role of XacFhaB regions as elicitors of plant defense responses was also analyzed. AR1, AR2 and AR3 at 5 μM, were infiltrated in citrus host plants as well as in non-host plants such as tomato and pepper. In pepper and tomato tissues infiltrated with AR1 and AR2 marked chlorotic lesions were observed and AR3-infiltrated tissues displayed necrotic lesions that were larger in tomato than in pepper leaves. In citrus infiltrated-leaves, AR1 caused no visible reaction while AR2 and AR3 both caused a mild chlorosis (Fig. 4a). Once again, when the proteins were boiled (without protein degradation) for 10 min previous to the infiltration in tomato leaves, the observed lesions almost disappeared (Fig. S2, see Supporting Information), suggesting that they require to be folded to exert their function. Further, callose deposition, a known marker for PAMP-triggered immunity (Nguyen *et al.*, 2010), was evaluated in the presence of the three regions at 6 hpi in tomato and pepper and at 16 hpi in citrus. The three regions induced significant callose deposition that was not displayed in the 6XHis-Trx-infiltrated control. A major response was observed in all AR3 infiltrated-leaves with a larger response for tomato than for pepper and citrus (Fig. 4b, c). Another marker of plant defense responses analyzed was the production of apoplastic reactive oxygen species (ROS). Infiltrations of the three XacFhaB regions in leaves elicited the production of hydrogen peroxide in citrus (6 hpi), pepper and tomato (1 hpi) as visualized by DAB staining (Fig. 4d). Infiltrations with the control 6XHis-Trx did not denote any DAB staining. Altogether these results show that the three identified regions

individually have varying potential to initiate the response, and therefore suggest a role for full XacFhaB in the induction of plant defense responses.

XacFhaB regions increase expression of genes for basal immune response

Then, the expression of genes involved in basal immune response was analyzed in citrus and in tomato, the non-host plant that showed the most significant phenotypes (Sgro *et al.*, 2012). For this purpose, leaves were infiltrated with 5 µM AR1, AR2, AR3 and buffer as a control. Plant RNA from infiltrated citrus and tomato tissues was extracted, and RT-qPCR was performed. In citrus leaves, the induction of several genes was observed in the presence of the three AR proteins (Fig. 5a). The induction of *MAPK3* and *WRKY30* was 2 to 3 times while *MKK4* was induced by the three regions more than 5 times ($p < 0.05$) (Fig. 5a). Consistent with the oxidative burst observed (Fig. 4d), *RbohB*, *GST*, *SOD* and *PrxA*, were also induced ($p < 0.05$). Finally, the defense-related proteins *Lox2* and *PR1* also showed increased expression, the latter only with AR2 and AR3 ($p < 0.05$), while *PR3* and *PR4* showed no significant changes (Fig. 5a). In tomato leaves, *MAPK3* and *MKK4* showed 2-fold induction with the three AR proteins at 1 hpi ($p < 0.05$). Also, the expression of two genes previously developed as markers for PTI in tomato such as *Gras2* and *Pti5* (Nguyen et al., 2010) was assayed showing a more than 3-fold induction with the three ARs ($p < 0.05$) (Fig. 5b).

Next, the ability of AR1, AR2 and AR3 to induce the expression of the recently identified CaHIR1 homologs in citrus and tomato leaves, as occurs with Fha1 from Xcv (Choi et al., 2013), was analyzed. With specific primers, transcript levels of *CsHIR* and *SlHIR* were quantified by RT-qPCR on RNA samples obtained from AR-infiltrated citrus and tomato leaves, respectively. The results showed that AR2 and AR3 induced HIR1 expression in both plants ($p < 0.05$), while AR1 did not (Fig. 5c).

Pre-infiltration of citrus leaves with XacFhaB regions impairs Xcc infection

Our results indicate that XacFhaB regions can promote defense responses in citrus leaves. Therefore, the potential effect of these regions to enhance canker disease resistance was investigated. Citrus leaves were pre-infiltratated with 1 μM of AR1, AR2 and AR3 and 6XHis-Trx as a control. The pre-infiltrated tissues were then infiltrated with Xcc at 10^6 CFU/ml and bacterial growth monitored up to 5 dpi. We observed that both at 3 and 5 dpi XacFhaB regions were able to induce a defense response reducing significantly ($p < 0.05$) the population of bacteria in the three cases (Fig. 6).

Further dissection of AR3, the region with the major eliciting activity

Considering the higher response observed for AR3 in the three plant species analyzed we dissected this region taking into account the information obtained by the Pfam analysis. Three subregions were expressed and purified as recombinant polypeptides in *E. coli* in view of the following: AR3-1 (2273-2448) encompasses only three type-1 hemagglutinin domains to analyze the minimal filamentous region, AR3-2 (2342-2576) that bears four type-1 hemagglutinin domains and predicts to adopt a larger filamentous structure than AR3-1, and AR3-3 (2709-3046) mainly composed by disordered predicted regions (Fig. 7a). The analysis of the responses of pepper, tomato and citrus leaves to these three AR3 subregions revealed that the three were able to elicit a response in pepper and tomato (Fig. 7b), while no response was observed in citrus leaves (data not shown), consistent with the mild chlorosis observed in these leaves when the complete AR3 was used (Fig. 4a). The production of hydrogen peroxide was analyzed by DAB staining in the three plant species (Fig. 7c). The three subregions caused hydrogen peroxide production in tomato and pepper. In citrus, AR3-2 and AR3-

3 denoted DAB staining while AR3-1 showed only a gentle reaction. Finally, the expression of characteristic basal immune response genes in tomato was analyzed by RT-qPCR (Fig. 7d). The results showed that MAPK3 and WRKY28 were induced with the three subregions ($p < 0.05$) while Pti5 expression was induced only with AR3-2 and AR3-3 ($p < 0.05$) and Gras2 showed no changes. Noticeably was the fact that none of them was able to increase the SlHIR expression (Fig. 7d).

DISCUSSION

Many bacterial pathogens have hemagglutinin proteins at their surfaces that allow them to adhere to the host tissue. The most studied among these proteins is FhaB from *B. pertussis*, which constitutes the pathogen's major adhesion factor for lung colonization. In fact, FhaB is one of the components of highly protective vaccines against whooping cough (Pines et al., 1999, Sato & Sato, 1999). FhaB is able to interact with complement receptor 3 (CR3) integrins of macrophages, crucial for pathogen phagocytosis (Mobberley-Schuman & Weiss, 2005) as well as to activate host interferon type I response (Dieterich & Relman, 2011). The fact that FhaB is an important adhesion factor and immune response activator led us to hypothesize that XacFhaB could have similar functions in plant infections. To perform the analyses and since full XacFhaB is a large protein difficult to express in *E. coli* as a recombinant protein, we dissected it in three regions.

Our results indicate that AR2 and AR3 are the main regions responsible for bacterial agglutination, and moreover, that the folded structures of AR2 and AR3 are required for the agglutination function. Considering mature XacFhaB as a long β-helical fiber spattered with flexible hinges as predicted and consistent with previous studies in *B. pertussis* FhaB, and being anchored through its N-terminal TPS domain, it is

reasonable that the more exposed regions AR2 and AR3 are those involved in adhesion, as we observed. Moreover, AR3 and its continuing Fha1-like region are predicted to be the most exposed ones in XacFhaB, resembling the most exposed region of *B. pertussis* FhaB and having the highest bacterial agglutination and defense elicitor activities (Mazar & Cotter, 2006). Notice that the lengths estimated for the mature, folded parts of these proteins are close to 0.05-0.06 micrometers, which are only 1-2 orders of magnitude smaller than bacterial sizes and could thus form thin layer of filaments covering the cells and reaching distances around 2-3% of their sizes (assuming a cell length of 2 μm) providing soft, flexible and sticky surfaces to facilitate unspecific adhesion.

We finally notice that processing of the precursor XacFhaB protein would not only lead to the full exposition of the last folded part that includes all the type-1 hemagglutinin domains and the Fha-1-like region, to mediate binding, but also the release of a disordered polypeptide of ~1,200 residues with type-2 hemagglutinin signatures. These domains have not been much characterized, but they compose a family of secreted bacterial exotoxins and as such could contribute with additional infective mechanisms to be explored.

The non-fimbrial plant pathogen adhesins share several characteristics observed in PAMP molecules previously characterized (Boller & Felix, 2009). Among them they are widely conserved in animal and plant pathogens, are localized at the outer membrane and are required for bacterial pathogenicity. Particularly, the idea that XacFhaB, as occurs with FhaB in animal hosts, may behave as an immune elicitor in plants is also supported by the recent evidence that Fha1 from Xcv that is 95 % identical to amino acids 3,067 to 3,508 of XacFhaB interacts with the positive regulator of pathogen-induced cell death CaHIR1 (Choi et al., 2013). In this context, we analyzed

markers of PTI response in tissues infiltrated with the different regions of XacFhaB. Phenotypical observation of cell death mainly in non-host plants tomato and pepper, callose deposition, DAB staining of ROS due to the oxidative burst produced during basal defense response and the induction of the expression of genes previously observed to be involved in basal defense response confirm that XacFhaB acts as a PAMP in the bacterial interaction with host and non-host tissue. We also analyzed the capacity of the different XacFhaB regions to induce HIR expression such as Fha1 of Xcv (Choi et al., 2013). In XacFhaB sequence, the homologous region to Fha1 begins 20 amino acids after AR3 carboxy-terminal end. Even so, AR2 and AR3 induced the expression of HIR1, suggesting that a large region of XacFhaB is able to be recognized by HIR1. AR1 did not induce the expression of HIR, this difference suggests that other membrane protein different from HIR1 may be interacting with XacFhaB regions ending in different outputs of the defense response.

A further confirmation of the role of the different XacFhaB regions triggering a plant defense response is the observation that the pre-infiltration of citrus leaves with these regions impair Xcc growth inducing citrus canker disease resistance. These results denote that XacFhaB regions may be used in a future as molecules to prevent canker development.

AR3 is the most reactive region of XacFhaB and this is consistent with the proposed folding model for FhaB of *B. pertussis* (Noel et al., 2012) that indicated that AR3 may be more exposed to the plant cell membranes. The goal of dissecting the AR3 in different structural-predicted different subregions was to further study this region. Like full AR3, the three subregions elicited a defense response and the main difference between the subregions and AR3 was the lack of HIR expression induction, suggesting a different regulated response to the subregions.

In summary, Xcc like other animal and plant bacterial pathogens requires proteins such as FhaB that let them adhere to host tissues and in the case of Xcc also to form a biofilm to complete the disease cycle and be able to colonize new niches (Gottig et al., 2009). However, our results demonstrate that plants have evolved strategies to recognize this virulence factor and thus hamper the disease process by mounting the basal PTI immune response. Particularly in the case of non-host plants this response is enough to hinder disease while in host plants due to Xcc pathogenic mechanisms, the bacteria can colonize the host and cause disease. Further studies about the plant molecules that could interact with XacFhaB regions will clarify how the plants could recognize this important Xcc virulence factor.

EXPERIMENTAL PROCEDURES

Strains, culture conditions and media

E. coli JM109 was used for DNA subcloning and cells were cultivated at 37°C in Luria Bertani (LB) medium. Xcc (Xcc99-1330) and the derivative *fhaB* mutant (ΔfhaB) were grown at 28°C in SB or XVM2 (Gottig et al., 2009). Antibiotics were used at the following final concentrations: ampicillin (Ap) 100 µg/ml for *E. coli* and 25 µg/ml for Xcc, kanamycin (Km) 40 µg/ml for both strains, gentamycin (Gm) 20 µg/ml for both strains and chloramphenicol (Cm) 30 µg/ml for *E. coli*. Xcc expressing the green fluorescence protein (GFP) was previously constructed (Gottig et al., 2009).

Expression and purification of recombinant FhaB regions

Regions AR1, AR2, AR3, AR3-1, AR3-2 and AR3-3 were amplified by PCR from Xcc genomic DNA by using the oligonucleotides AR1LB and AR1RH, AR2LB and AR2RH, AR3LB and AR3RH, AR3-1LB and AR3-1RH, AR3LB and AR3-2RH, AR3-3LB and AR3RH, respectively (Table S1, see Supporting Information) and cloned into

pET28a vector (Novagen) previously digested with the restriction enzymes *BamH*I and *Hind*III. After transformation into *E. coli* strain BL21 (pLysS), synthesis of recombinant polypetides and also of 6XHis-Trx (Thioredoxin) was induced by IPTG 0.1 mM for 16 h at 18°C. The proteins were purified by affinity from the soluble fraction of the bacterial lysates by using Ni-NTA agarose (Qiagen, Hilden, Germany). The purity of recombinant proteins was checked by SDS-PAGE.

Plant material and plant infiltrations

Citrus sinensis cv. Valencia were grown in a green house at 26 ± 2°C and tomato (*Solanum lycopersicum* cv. Victoria) and pepper (*Capsicum annuum* cv. Grossum) at 24 ± 2°C, all of them with a photoperiod of 16 h. Proteins were infiltrated with needleless syringes at 5 μM. Bacteria were grown in SB broth to an optical density of 1 at 600 nm, harvested by centrifugation, and resuspended in 10 mM $MgCl_2$ at the required density. Infiltrations into leaves were performed with needleless syringes.

Bacterial aggregation assays

For bacterial aggregation assays, 20 μl of cultured Xcc expressing GFP were incubated with or without 5 μM of each of XacFhaB regions for 3 h on glass slides in a humidity chamber. Then, bacteria were visualized by confocal laser scanning microscopy (Nikon Eclipse TE-2000-E2).

Callose staining and DAB staining

The callose staining was done as previously described (Sgro et al., 2012) and examined by confocal laser scanning microscopy (Nikon Eclipse TE-2000-E2). Average callose measurements were based on at least 20 photographs from three independent experiments, and were analysed for statistical differences by one-way ANOVA ($p < 0.05$). DAB staining was done as previously described (Piazza *et al.*, 2015). Cleared leaves were observed and photographed in an optical microscope.

RNA preparation and Real-Time PCR

Total RNA was isolated from plant infiltrated leaves using TRIzol® reagent (Invitrogen, USA) according to the manufacturer's instructions. At least 100 mg of frozen tissue was used for each total RNA extraction and samples were stored at -80 ºC until used. The RT-qPCRs were performed as previously described (Sgro et al., 2012). Oligonucleotides designed on defense-associated genes were used to amplify the tomato and citrus transcripts. As control, the oligonucleotides for the ribosomal protein L2 (Rpl2) were used in tomato and in the case of citrus for actin (Table S1, see Supporting Information). The primers used for tomato (Wei *et al.*, 2015) and citrus (Piazza et al., 2015) were previously used and detailed in (Table S1, see Supporting Information). Oligonucleotides for the amplification of HIR genes in both species were designed looking for the homologs of pepper HIR (CaHIR). Gene specific cDNA amounts were calculated from threshold cycle (Ct) values, expressed as relative to controls, and normalized with respect to actin cDNA, used as internal reference. Values were normalized by an internal reference (Ct_r) according to the equation $\Delta Ct = Ct - Ct_r$ and quantified as $2^{-\Delta Ct}$. A second normalization by a control (Ct_c) $\Delta\Delta Ct = Ct - Ct_c$ produces a relative quantification: $2^{-\Delta\Delta Ct}$. The results were analyzed with one-way analysis of variance (ANOVA).

Analysis of Xcc growth in citrus leaves pre-infiltrated the different XacFhaB regions

Citrus leaves were pre-infiltrated with needleless syringes with purified 6XHis-Trx and the different XacFhaB regions at 1 μM. After 16 h these leaves were infiltrated with Xcc suspension at 10^6 CFU/ml. Growth assays were performed at 0, 3 and 5 dpi from 10 infiltrated leaves for each treatment at the indicated times by grinding 0.8 cm diameter leaf discs in 1 ml of 10 mM $MgCl_2$, followed by serial dilutions, and plating

onto SB agar plates. Colonies were counted after 48 h of incubation at 28ºC, and the results are presented as log of CFU per cm^2 of leaf tissue. In all cases, data were statically analyzed by one-way ANOVA ($p < 0.05$).

ACKNOWLEDGMENTS

We thank Rodrigo Vena for assistance with the microscopy confocal facility, Catalina Anderson (INTA Concordia, Argentina), Gastón Alanis and Rubén Díaz Vélez (Proyecto El Alambrado) for the citrus plants and Diego Aguirre for plant technical assistance. This work was supported by grants from Argentine Federal Government (PICT2013-0625 to JO and PICT2013-0556 to NG). BSG, JO and NG are staff members of the Consejo Nacional de Investigaciones Científicas y Técnicas (CONICET, Argentina).

REFERENCES

Amano, A. (2010) Bacterial adhesins to host components in periodontitis. *Periodontol 2000,* **52,** 12-37.

Boller, T. and Felix, G. (2009) A renaissance of elicitors: perception of microbe-associated molecular patterns and danger signals by pattern-recognition receptors. *Annu Rev Plant Biol,* **60,** 379-406.

Clantin, B., Hodak, H., Willery, E., Locht, C., Jacob-Dubuisson, F. and Villeret, V. (2004) The crystal structure of filamentous hemagglutinin secretion domain and its implications for the two-partner secretion pathway. *Proc Natl Acad Sci U S A,* **101,** 6194-6199.

Coletta, A., Pinney, J.W., Solis, D.Y., Marsh, J., Pettifer, S.R. and Attwood, T.K. (2010) Low-complexity regions within protein sequences have position-dependent roles. *BMC Syst Biol,* **4,** 43.

Chisholm, S.T., Coaker, G., Day, B. and Staskawicz, B.J. (2006) Host-microbe interactions: shaping the evolution of the plant immune response. *Cell,* **124,** 803-814.

Choi, H.W., Kim, D.S., Kim, N.H., Jung, H.W., Ham, J.H. and Hwang, B.K. (2013) Xanthomonas filamentous hemagglutinin-like protein Fha1 interacts with pepper hypersensitive-induced reaction protein CaHIR1 and functions as a virulence factor in host plants. *Mol Plant Microbe Interact,* **26,** 1441-1454.

Dieterich, C. and Relman, D.A. (2011) Modulation of the host interferon response and ISGylation pathway by B. pertussis filamentous hemagglutinin. *PLoS One,* **6,** e27535.

Garavaglia, B.S., Thomas, L., Gottig, N., Dunger, G., Garofalo, C.G., Daurelio, L.D., *et al.* (2010) A eukaryotic-acquired gene by a biotrophic phytopathogen allows prolonged survival on the host by counteracting the shut-down of plant photosynthesis. *PLoS One,* **5,** e8950.

Gottig, N., Garavaglia, B.S., Garofalo, C.G., Orellano, E.G. and Ottado, J. (2009) A filamentous hemagglutinin-like protein of Xanthomonas axonopodis pv. citri, the phytopathogen responsible for citrus canker, is involved in bacterial virulence. *PLoS One,* **4,** e4358.

Graham, J.H., Gottwald, T.R., Cubero, J. and Achor, D.S. (2004) Xanthomonas axonopodis pv. citri: factors affecting successful eradication of citrus canker. *Mol Plant Pathol,* **5,** 1-15.

Julio, S.M., Inatsuka, C.S., Mazar, J., Dieterich, C., Relman, D.A. and Cotter, P.A. (2009) Natural-host animal models indicate functional interchangeability between the filamentous haemagglutinins of Bordetella pertussis and Bordetella bronchiseptica and reveal a role for the mature C-terminal domain, but not the RGD motif, during infection. *Mol Microbiol,* **71,** 1574-1590.

Kajava, A.V., Cheng, N., Cleaver, R., Kessel, M., Simon, M.N., Willery, E., *et al.* (2001) Beta-helix model for the filamentous haemagglutinin adhesin of Bordetella pertussis and related bacterial secretory proteins. *Mol Microbiol,* **42,** 279-292.

Mazar, J. and Cotter, P.A. (2006) Topology and maturation of filamentous haemagglutinin suggest a new model for two-partner secretion. *Mol Microbiol,* **62,** 641-654.

Mhedbi-Hajri, N., Jacques, M.A. and Koebnik, R. (2011) Adhesion mechanisms of plant-pathogenic Xanthomonadaceae. *Adv Exp Med Biol,* **715,** 71-89.

Mobberley-Schuman, P.S. and Weiss, A.A. (2005) Influence of CR3 (CD11b/CD18) expression on phagocytosis of Bordetella pertussis by human neutrophils. *Infect Immun,* **73,** 7317-7323.

Nguyen, H.P., Chakravarthy, S., Velasquez, A.C., McLane, H.L., Zeng, L., Nakayashiki, H., *et al.* (2010) Methods to study PAMP-triggered immunity using tomato and Nicotiana benthamiana. *Mol Plant Microbe Interact,* **23,** 991-999.

Noel, C.R., Mazar, J., Melvin, J.A., Sexton, J.A. and Cotter, P.A. (2012) The prodomain of the Bordetella two-partner secretion pathway protein FhaB remains intracellular yet affects the conformation of the mature C-terminal domain. *Mol Microbiol,* **86,** 988-1006.

Piazza, A., Zimaro, T., Garavaglia, B.S., Ficarra, F.A., Thomas, L., Marondedze, C., *et al.* (2015) The dual nature of trehalose in citrus canker disease: a virulence factor for Xanthomonas citri subsp. citri and a trigger for plant defence responses. *J Exp Bot,* **66,** 2795-2811.

Pines, E., Barrand, M., Fabre, P., Salomon, H., Blondeau, C., Wood, S.C., *et al.* (1999) New acellular pertussis-containing paediatric combined vaccines. *Vaccine,* **17,** 1650-1656.

Rado-Trilla, N. and Alba, M. (2012) Dissecting the role of low-complexity regions in the evolution of vertebrate proteins. *BMC Evol Biol,* **12,** 155.

Roy, A., Kucukural, A. and Zhang, Y. (2010) I-TASSER: a unified platform for automated protein structure and function prediction. *Nat Protoc,* **5,** 725-738.

Sato, Y. and Sato, H. (1999) Development of acellular pertussis vaccines. *Biologicals,* **27,** 61-69.

Sgro, G.G., Ficarra, F.A., Dunger, G., Scarpeci, T.E., Valle, E.M., Cortadi, A., *et al.* (2012) Contribution of a harpin protein from Xanthomonas axonopodis pv. citri to pathogen virulence. *Mol Plant Pathol,* **13,** 1047-1059.

Wei, T., Wang, L., Zhou, X., Ren, X., Dai, X. and Liu, H. (2015) PopW activates PAMP-triggered immunity in controlling tomato bacterial spot disease. *Biochem Biophys Res Commun*.

Yang, J., Yan, R., Roy, A., Xu, D., Poisson, J. and Zhang, Y. (2015) The I-TASSER Suite: protein structure and function prediction. *Nat Methods,* **12,** 7-8.

Zhang, Y. (2008) I-TASSER server for protein 3D structure prediction. *BMC Bioinformatics,* **9,** 40.

SUPPORTING INFORMATION LEGENDS

Fig. S1. XacFhaB sequence alignments. The sequences of XacFhaB and Fha1 from Xcv **(a)** and AR2 and AR2' **(b)** were aligned with ClustalW2.

Fig. S2. The response of tomato leaves infiltrated with AR1, AR2 and AR3 requires the polypeptides to be folded. Representative photographs of the responses 1 dpi to the infiltration of 5 μM AR1, AR2 and AR3 at room temperature and previously boiled for 10 min. Bar indicates 1 mm.

Table S1. Oligonucleotides used in this study

FIGURE LEGENDS

Fig. 1. Analysis of the expression levels of genes related with defense responses in citrus leaves infected with Xcc and the ΔfhaB mutant by RT-qPCR. RNA extracted from citrus leaves 1 day post infiltration (dpi) with Xcc and ΔfhaB mutant was subjected to RT-qPCR of citrus genes related with defense responses. White bars indicate the expression levels observed for Xcc-infected samples and grey bars indicate the expression levels of the mutant relativized to the wild type. Values are the means of three biological replicates with three technical replicates each. Error bars indicate standard deviations. Results were analyzed by one-way ANOVA ($p < 0.05$).

Fig. 2. Schematic representation and modeling of FhaB. (a) Schematic representation of Xcc FhaB. The dark blue box indicates the signal peptide, the light blue box is the TPS domain. AR1, AR2 and AR3 are indicated as green, yellow and purple boxes, with their lengths indicated inside. The light pink box indicates a region highly similar to Xcv Fha1. The pink arrow indicates the putative protease-processing site. Red and blue boxes below the representation of the full protein show type-1 and type-2 Filamentous Hemagglutinin signatures, respectively, as detected by PFAM. **(b)** Disorder predictions by the PrDOS server for XacFhaB. This plot is aligned to the diagram shown in panel A. **(c)** Schematic representation of XacFhaB's structure, based on the disorder predictions and on partial modeling of 600 residue-long segments with the I-TASSER server: The first ~3500 residues are predicted to form a large flexible β-fiber, while the whole segment C-terminal to the processing site is expected to be highly disordered.

Fig. 3. Analysis of the ability of AR1, AR2 and AR3 to aggregate Xcc cells. Representative photographs of confocal laser scanning microscopy of GFP-expressing Xcc wild-type in the presence of 5 µM AR1, AR2 and AR3. As control (C), 6XHis-Trx was used. Bar, 10 µm.

Fig. 4. Analysis of the responses in pepper, tomato and citrus leaves infiltrated with AR1, AR2 and AR3. (a) Representative photographs of the responses 1 dpi to the infiltration of 5 µM AR1, AR2 and AR3. Bar indicates 1 mm. **(b)** Representative fluorescence microscopy photographs of Aniline blue staining of callose deposition in pepper and tomato leaves 6 hpi and citrus 16 hpi. Bar indicates 20 µm. **(c)** Relative callose intensities were quantified as described in Experimental Procedures. Values

represent means standardized to the mean callose intensity in control-treated leaves. Error bars indicate standard deviations. The results are representative of three independent experiments. Results were analyzed by one-way ANOVA ($p < 0.05$). **(d)** Representative photographs of DAB staining leaves in pepper, tomato and citrus leaves infiltrated with the three XacFhaB regions (1 hpi pepper and tomato and 6 hpi for citrus leaves). Bars in (b) and (d) are 1 mm. In all cases 6XHis-Trx was used as control.

Fig. 5. Analysis of the expression levels of genes related with defense responses in citrus and tomato leaves infiltrated with AR1, AR2 and AR3 by RT-qPCR. (a) RNA was extracted from citrus leaves 16 hpi or **(b)** tomato 6 hpi. **(c)** Relative expression levels of CsHIR and SlHIR in citrus and tomato leaves infiltrated with AR1, AR2 and AR3, respectively. Bars indicate the expression levels of the genes relative to the expression levels of the buffer-infiltrated control. Values are the means of four biological replicates with three technical replicates each. Error bars indicate standard deviations. Results were analyzed by one-way ANOVA ($p < 0.05$).

Fig. 6. Analysis of Xcc growth in citrus leaves pre-infiltrated with AR1, AR2 and AR3. Quantification of Xcc growth in citrus leaves pre-infiltrated with 1 μM of AR1, AR2 and AR3, or with 6XHis-Trx as control. Values are the means obtained from 10 infiltrated citrus leaves at different dpi. Error bars show the standard deviation. Results were analyzed by one-way ANOVA ($p < 0.05$).

Fig. 7. Analysis of the responses in tomato leaves infiltrated with AR3-1, AR3-2 and AR3-3. (a) Schematic representation of XacFhaB AR3 sub-regions. Numbers indicate amino acids in the full length protein. **(b)** Representative photographs of the

responses 1 dpi to the infiltration of 5 µM AR3-1, AR3-2 and AR3-3 in tomato and pepper. **(c)** DAB detection of H_2O_2 accumulation in tomato leaves infiltrated with AR3-1, AR3-2 and AR3-3 1 dpi. Representative photographs of DAB staining leaves. Bars indicates 1 mm. **(d)** RT-qPCR of tomato genes related with defense responses. Bars indicate the expression levels relative to control of the genes from RNA extracted from leaves infiltrated with AR3 subregions at 1 dpi. Values are the means of four biological replicates with three technical replicates each. Error bars indicate standard deviations. Results were analyzed by one-way ANOVA ($p < 0.05$).

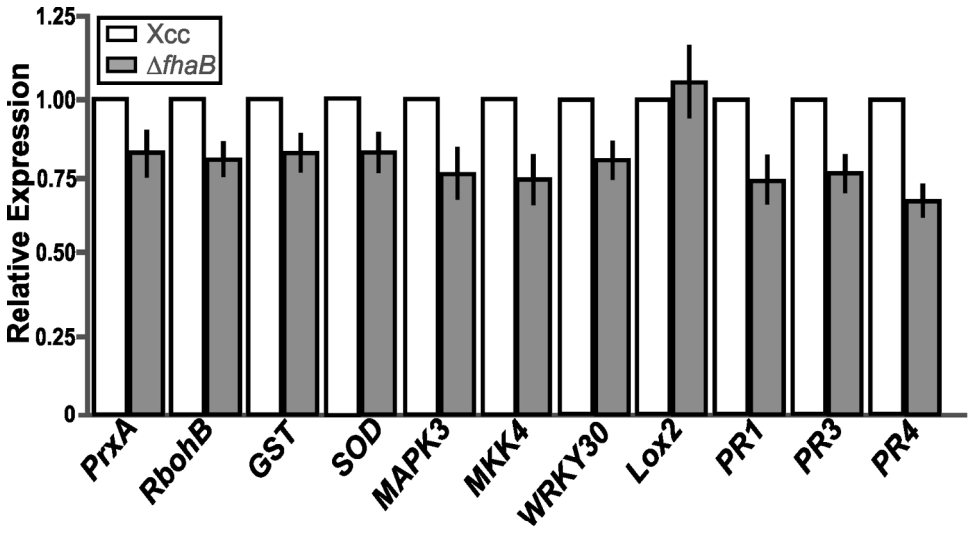

Fig. 1. Analysis of the expression levels of genes related with defense responses in citrus leaves infected with Xcc and the ΔfhaB mutant by RT-qPCR. RNA extracted from citrus leaves 1 day post infiltration (dpi) with Xcc and ΔfhaB mutant was subjected to RT-qPCR of citrus genes related with defense responses. White bars indicate the expression levels observed for Xcc-infected samples and grey bars indicate the expression levels of the mutant relativized to the wild type. Values are the means of three biological replicates with three technical replicates each. Error bars indicate standard deviations. Results were analyzed by one-way ANOVA ($p < 0.05$).

166x119mm (300 x 300 DPI)

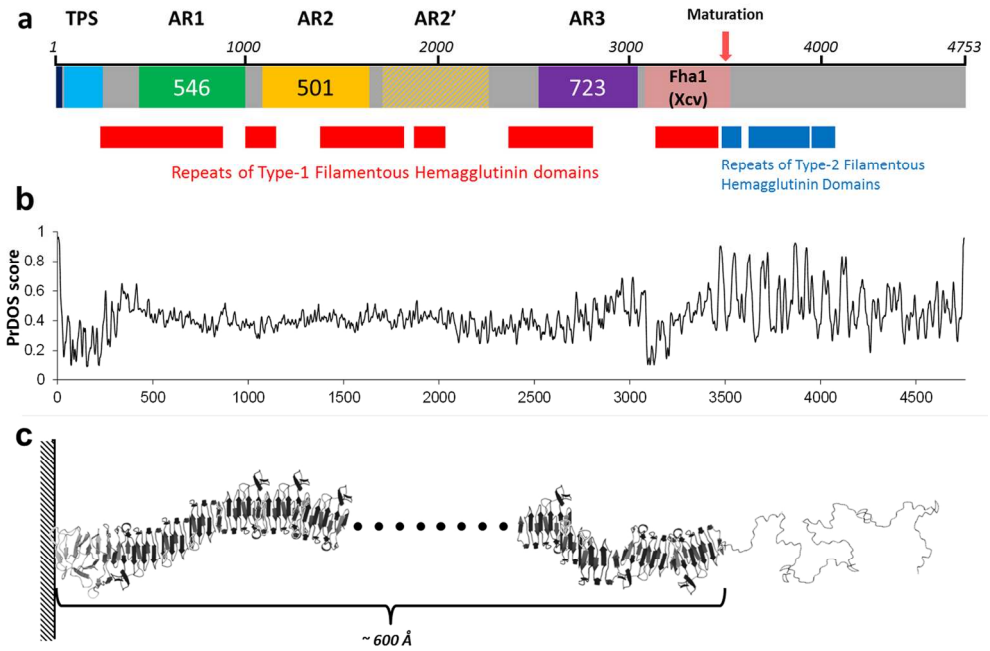

Fig. 2. Schematic representation and modeling of FhaB. (a) Schematic representation of Xcc FhaB. The dark blue box indicates the signal peptide, the light blue box is the TPS domain. AR1, AR2 and AR3 are indicated as green, yellow and purple boxes, with their lengths indicated inside. The light pink box indicates a region highly similar to Xcv Fha1. The pink arrow indicates the putative protease-processing site. Red and blue boxes below the representation of the full protein show type-1 and type-2 Filamentous Hemagglutinin signatures, respectively, as detected by PFAM. (b) Disorder predictions by the PrDOS server for XacFhaB. This plot is aligned to the diagram shown in panel A. (c) Schematic representation of XacFhaB's structure, based on the disorder predictions and on partial modeling of 600 residue-long segments with the I-TASSER server: The first ~3500 residues are predicted to form a large flexible β-fiber, while the whole segment C-terminal to the processing site is expected to be highly disordered.
166x114mm (300 x 300 DPI)

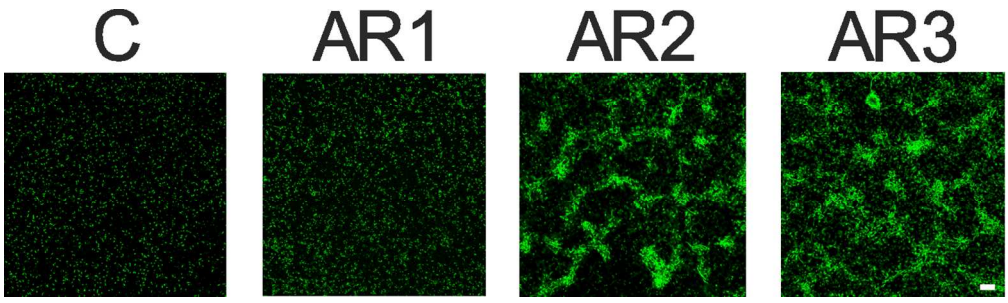

Fig. 3 Analysis of the ability of AR1, AR2 and AR3 to aggregate Xcc cells. Representative photographs of confocal laser scanning microscopy of GFP-expressing Xcc wild-type in the presence of 5 μM AR1, AR2 and AR3. As control (C), 6XHis-Trx was used. Bar, 10 μm.
123x35mm (300 x 300 DPI)

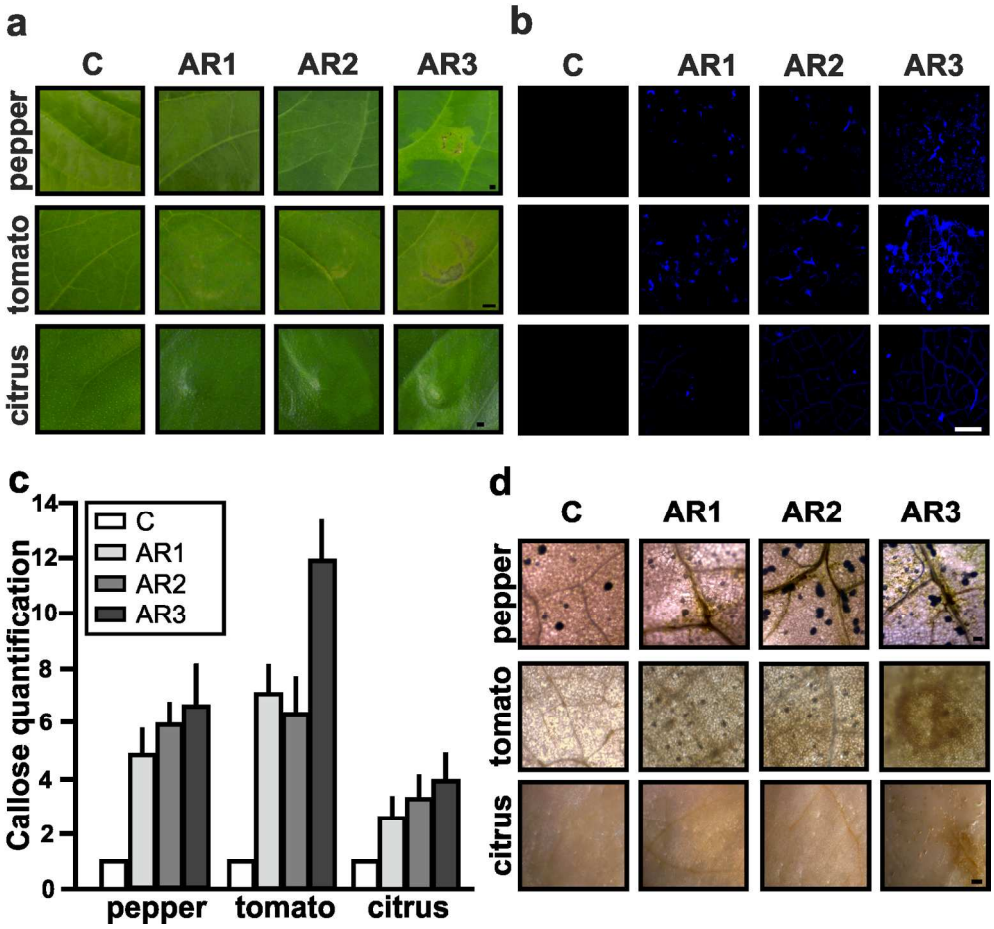

Fig. 4. Analysis of the responses in pepper, tomato and citrus leaves infiltrated with AR1, AR2 and AR3. (a) Representative photographs of the responses 1 dpi to the infiltration of 5 μM AR1, AR2 and AR3. Bar indicates 1 mm. (b) Representative fluorescence microscopy photographs of Aniline blue staining of callose deposition in pepper and tomato leaves 6 hpi and citrus 16 hpi. Bar indicates 20 μm. (c) Relative callose intensities were quantified as described in Experimental Procedures. Values represent means standardized to the mean callose intensity in control-treated leaves. Error bars indicate standard deviations. The results are representative of three independent experiments. Results were analyzed by one-way ANOVA ($p < 0.05$). (d) Representative photographs of DAB staining leaves in pepper, tomato and citrus leaves infiltrated with the three XacFhaB regions (1 hpi pepper and tomato and 6 hpi for citrus leaves). Bars in (b) and (d) are 1 mm. In all cases 6XHis-Trx was used as control.
164x152mm (300 x 300 DPI)

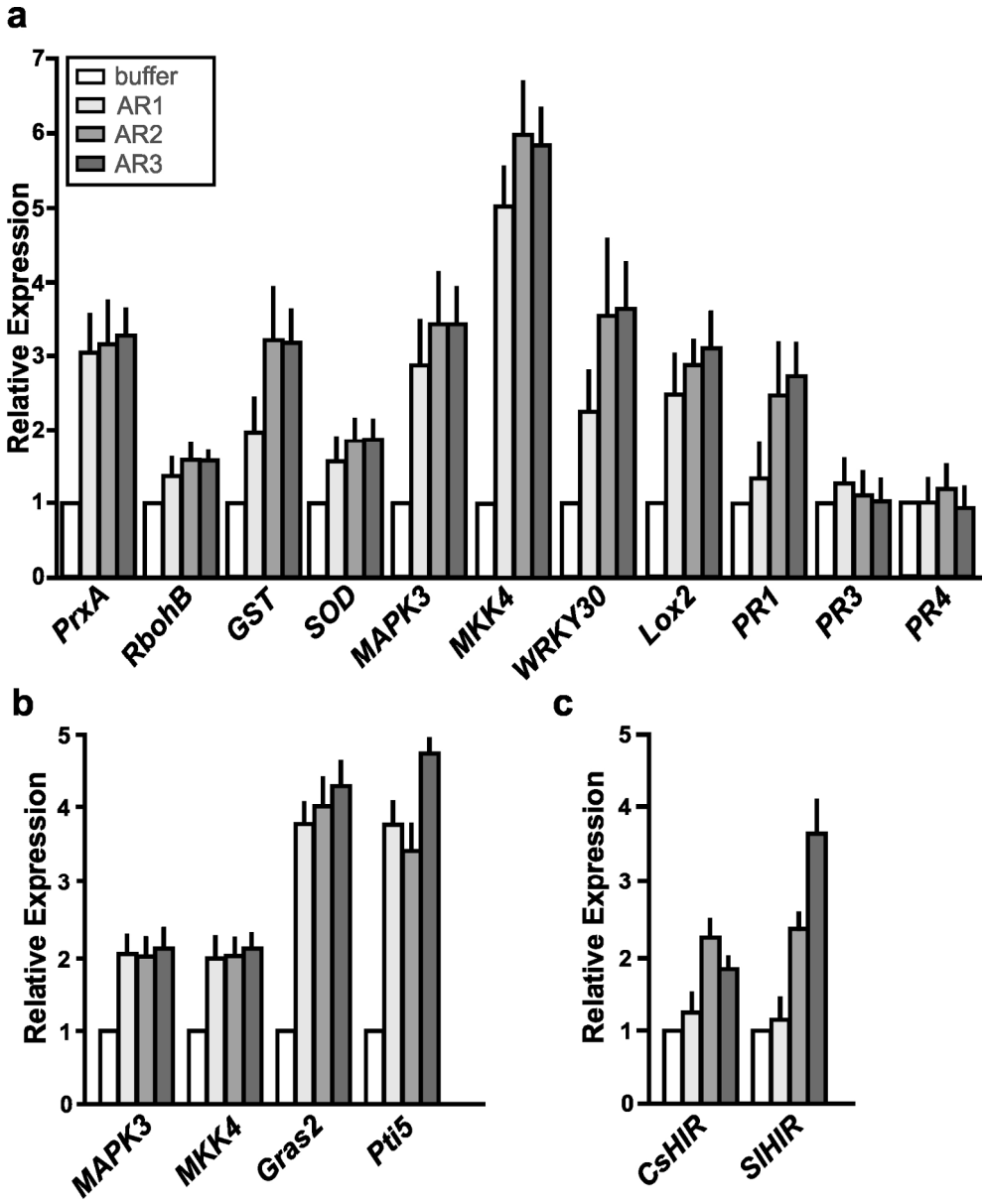

Fig. 5. Analysis of the expression levels of genes related with defense responses in citrus and tomato leaves infiltrated with AR1, AR2 and AR3 by RT-qPCR. (a) RNA was extracted from citrus leaves 16 hpi or (b) tomato 6 hpi. (c) Relative expression levels of CsHIR and SlHIR in citrus and tomato leaves infiltrated with AR1, AR2 and AR3, respectively. Bars indicate the expression levels of the genes relative to the expression levels of the buffer-infiltrated control. Values are the means of four biological replicates with three technical replicates each. Error bars indicate standard deviations. Results were analyzed by one-way ANOVA ($p < 0.05$).
167x205mm (300 x 300 DPI)

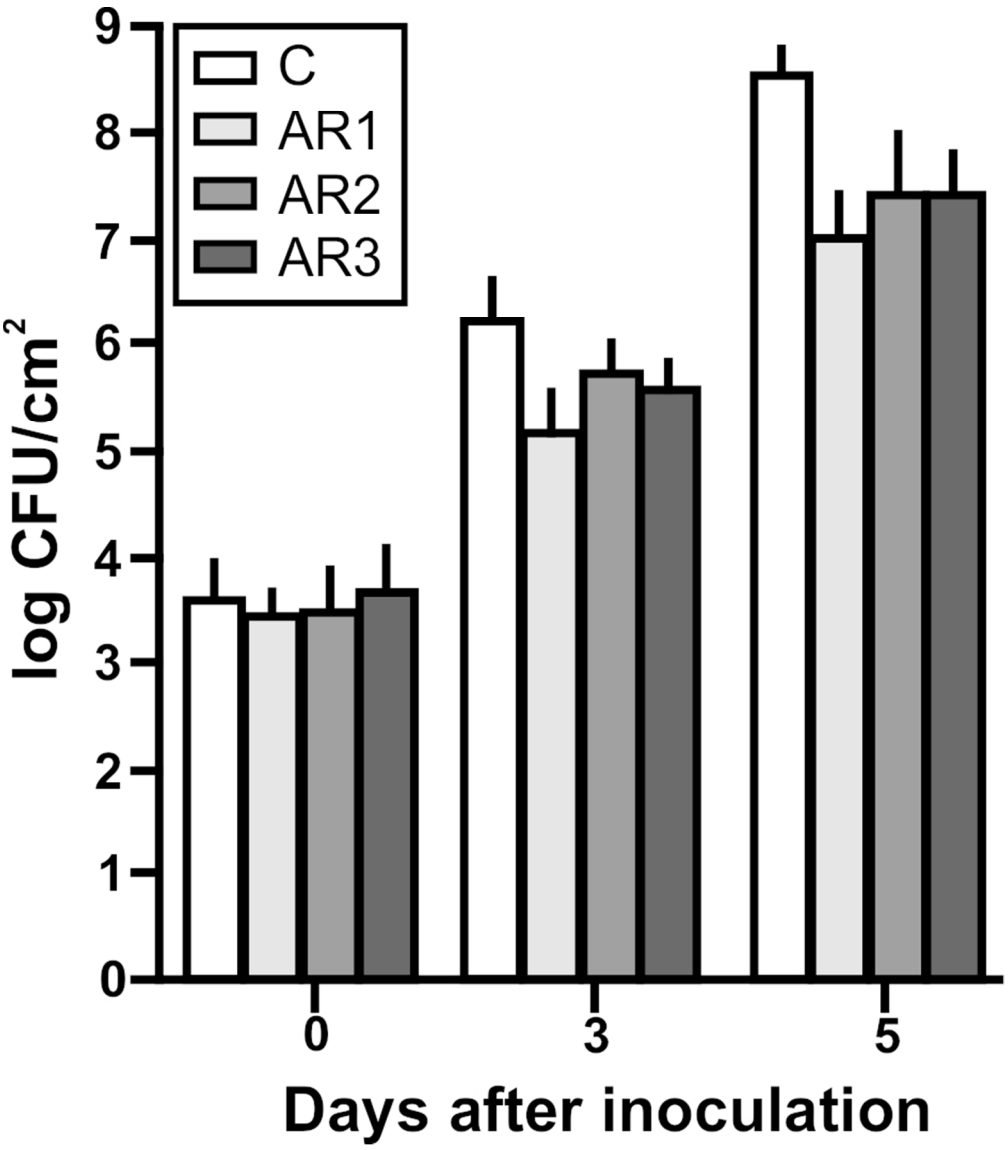

Fig. 6. Analysis of Xcc growth in citrus leaves pre-infiltrated with AR1, AR2 and AR3. Quantification of Xcc growth in citrus leaves pre-infiltrated with 1 μM of AR1, AR2 and AR3, or with 6XHis-Trx as control. Values are the means obtained from 10 infiltrated citrus leaves at different dpi. Error bars show the standard deviation. Results were analyzed by one-way ANOVA ($p < 0.05$).

79x90mm (300 x 300 DPI)

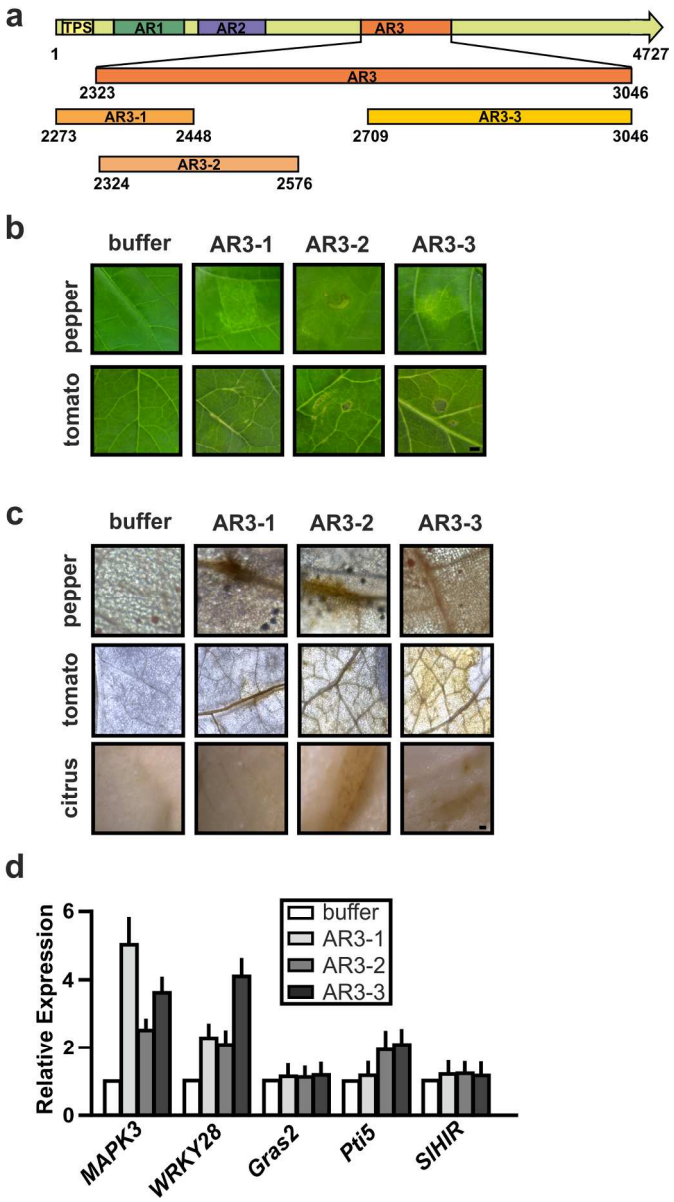

Fig. 7. Analysis of the responses in tomato leaves infiltrated with AR3-1, AR3-2 and AR3-3. (a) Schematic representation of XacFhaB AR3 sub-regions. Numbers indicate amino acids in the full length protein. (b) Representative photographs of the responses 1 dpi to the infiltration of 5 μM AR3-1, AR3-2 and AR3-3 in tomato and pepper. (c) DAB detection of H2O2 accumulation in tomato leaves infiltrated with AR3-1, AR3-2 and AR3-3 1 dpi. Representative photographs of DAB staining leaves. Bars indicates 1 mm. (d) RT-qPCR of tomato genes related with defense responses. Bars indicate the expression levels relative to control of the genes from RNA extracted from leaves infiltrated with AR3 subregions at 1 dpi. Values are the means of four biological replicates with three technical replicates each. Error bars indicate standard deviations. Results were analyzed by one-way ANOVA ($p < 0.05$).
129x229mm (300 x 300 DPI)